A Mathematical Model for Control of an Autonomous Vehicle Convoy

Plamen Petrov
Faculty of Mechanical Engineering,
Technical University of Sofia
8, Kl. Ohridski str., 1797 Sofia
BULGARIA
e-mail: ppetrov@tu-sofia.bg

Abstract: - This paper describes the modeling of a two-vehicle convoy and the design of a vehicle following controller that tracks the trajectory of the vehicle ahead with prescribed inter-vehicle distance. Kinematic equations of the system are formulated applying standard robotic methodology. We consider autonomous vehicle following without any information obtained from road infrastructure or communicated from the lead vehicle. Assuming that the leader linear and angular velocities, as well the curvature radius of the path traveled by the lead vehicle, are unknown constant parameters, an adaptive tracking controller is proposed. With only the current inter-vehicle relative position and orientation available for feedback control, the control velocities of the following vehicle are computed using the leader velocity estimates obtained from the dynamic (adaptive) part of the proposed controller. For constant velocity maneuvers of the leader, at steady state, the two-vehicle convoy will travel concentric arcs of same radii with prescribed inter-vehicle spacing. For time-varying lead vehicle velocities, the proposed controller achieves ultimate boundness of the closed-loop system in error coordinate. Various simulation results demonstrating the performance of the controller are included.

Key-Words: - Autonomous vehicle convoy, vehicle following, kinematic model, nonlinear adaptive control

1 Introduction

In recent years, the problem of automatic vehicle following in a convoy-like fashion, where each vehicle tracks the path taken by the preceding car at a desired separation distance, has attracted a considerable interest. The research effort into vehicle platooning and automatic vehicle following is based on the fact that often multiple vehicles have the possibility of solving transportation problems more efficiently than a single vehicle. This scenario is very useful in the case of military convoys [1]-[3], convoys of commercial vehicles [4], [7], personal vehicles [6] or in the public urban transport [5], [8].

Lateral (steering) control and longitudinal (spacing and speed) control were initially designed as two separate control systems. Each controller was designed as if the longitudinal and the steering vehicle dynamics were independent. Much research has been done in the study of longitudinal control of a platoon of vehicles on a straight line with different spacing policies [9]. For the lateral control of a vehicle convoy two basic concepts are studied. In [10], the lateral control is focused on the concept of cooperation between the vehicle and the road. The lane keeping performance relies on suitable reference markers and communication infrastructure to supply the vehicle with information about the road geometry. As an alternative, the concept of autonomous vehicle following [6], implies that the ego-vehicle tracks the trajectory of the vehicle ahead instead of the road by using on-board sensors that detect the vehicle relative position with respect to the lead vehicle. One of the principle issues in designing controllers for autonomous vehicle following is to determine the desired trajectory of the following vehicle. Previous work in generating the desired trajectory for the ego-vehicle has used several approaches including "trajectory-based approach", [11] that uses the time history of the lead vehicle, i.e., the ego-vehicle has to follow the path of the leader, not the lead vehicle itself. In [7], a tracking method involves using a contour of constant curvature to interpolate a trajectory between the following and the lead vehicle. In [12], a direct control of the following vehicle using information from on-board sensing without inter-vehicle communication has been proposed. A different approach to vehicle following control by using inter-vehicle communication has also been used, [13]. An interesting solution is the use of

RTK GPS sensors, which can provide in real time localization with high accuracy, [14]. In combination with inter-vehicle communication, these sensors permit to interchange absolute localization measurements.

In this paper, we consider the problem of autonomous vehicle following without the use of road infrastructure or inter-vehicle communication. The only information the following (robot) vehicle can use for feedback control is the current relative position and orientation with respect to the lead vehicle obtained from onboard sensors, which monitor the rear end of the lead vehicle.

Our contributions in this paper are two-fold: the control algorithms and the use of robotic oriented approach to mathematical leader/follower modeling that allow the following vehicle to track the path taken by the lead vehicle at a specific position in the plan with respect to the leader, and in the presence of unknown leader linear and angular velocities, as well the curvature radius of the path traveled by the lead vehicle.

One of the objectives of this paper is to develop a mathematical model of a vehicle convoy suitable for feedback control design. We formulate the kinematic equations of a two-vehicle convoy in error coordinates applying standard robotic methodology.

One of the challenges in designing controllers for automatic vehicle tracking is to decide on the desired trajectory of the following vehicle. On a curved road section, traveling an arc concentric to that traveled by the lead car but with bigger or smaller radius may be unacceptable from a practical point of view, (for example, the problem of "cutting the corner"). Assuming that the lead vehicle linear and angular velocities are unknown constant parameters, and the curvature radius of the path taken by the lead vehicle is also unknown, we are interested in designing a controller for the following vehicle, such that, at steady state, the following vehicle tracks the path taken by the lead vehicle with prescribed inter-vehicle distance. The approach used in this paper is closely related to that presented in [12] in the sense that it consists in tracking a reference virtual point, which is positioned at a desired known distance behind the lead vehicle with a virtual reference point located at a desired distance ahead of the following vehicle. This approach has been inspired from our previous work [15] concerning the problem of controlling a LHD (Load-Haul-Dump) vehicle. At steady-state, the two linked units of the LHD vehicle with equal unit length will travel concentric arcs of same radii. In this paper, the adaptive control designed is based on a reduced order dynamics and achieves asymptotic stabilization of the closed-loop system in error coordinates. The control velocities (control inputs) of the following vehicle are computed using the leader velocity estimates obtained from the dynamic (adaptive) part of the controller, which was designed as a parameter update law. The stability of the internal dynamics is also analyzed. There has also been attention paid to the evaluation of the performance of the adaptive controller, if the velocities of the lead vehicle are time-varying instead of constant parameters. Throughout this paper, feedback control design and stability analysis are performed via Lyapunov techniques.

The organization of this paper is as follows: in Section II, the development of the mathematical model of the vehicle convoy suitable for feedback control is presented. The problem formulation is given in Section III. In Section IV, the adaptive tracking controller of the two-vehicle convoy is proposed. Section V contains simulation results which illustrate the effectiveness of the proposed controller. Conclusions are presented in Section VI.

2 Kinematic Modeling

2.1 Vehicle Kinematic Model

2.1.1 Coordinate System Assignments

In this section, we apply standard robotic nomenclature for translational and rotational displacements and velocities, and methodology [16] to model the kinematics of the vehicle in the convoy. Fig. 1 depicts the schematic of the vehicles considered in this paper. From now on, the index *i=1* corresponds to the lead vehicle, and *i=2* corresponds to the following vehicle in the platoon. The vehicle has four non-deformable wheels. The wheels are assumed to roll on a horizontal plane without slipping. The longitudinal base A_iB_i of the vehicle is denoted by l_i , *(i=1,2),* To simplify the derivation of the vehicle control algorithms, we a use a planar bicycle 2DOFs vehicle model where two virtual wheels are located at the midpoints of the front and rear wheel axles, (Fig. 1). Although these two wheels do not exist, it is assumed that they comply with the wheel rolling without slipping conditions.

To describe the position and orientation of the vehicle in the plane, we assign the following coordinate frames (Fig. 1).

- $A_i x_{Ai} y_{Ai}$: Vehicle coordinate system located at the center of the rear vehicle axle and stationary with respect to the vehicle body; the x_{Ai} axis is along the longitudinal base of the vehicle, ($i=1, 2$).
- $B_i x_i y_i$: Wheel coordinate system with origin placed at the center of the front steering wheel; the x_i axis is in the direction of the wheel orientation, ($i=1, 2$).
- Fxy denotes an inertial coordinate frame in the plane to travel.

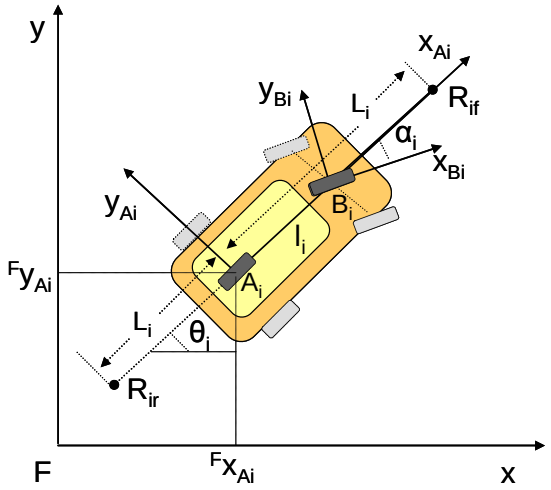

Fig. 1. Schematic of the vehicle

The coordinates of a reference point A_i placed at the center of the rear vehicle axle, with respect to an inertial frame *Fxy*, are denoted by $({}^F x_{Ai}, {}^F y_{Ai})$. The angle θ_i is the orientation angle of the vehicle with respect to the frame *Fxy*. The angle α_i, is the front wheel steering angle. The steering angle is measured with respect to the vehicle body. The reference points R_{1r} and R_{2f} located on the longitudinal vehicle axle are associated with the lead and following vehicle, respectively. The point R_{1r} is placed a L_1 distance behind point A_1 of the lead vehicle and point R_{2f} is placed a L_2 distance in front of point A_2 of the following vehicle.

Since the vehicle is assumed to move on a planar surface, in what follows, we use 3x3 rather than *4x4* homogeneous transformation matrices ${}^A T_B$ to transform the coordinates of a point S in coordinate frame B denoted by ${}^B p_S$ to its corresponding coordinates ${}^A p_S$ in the coordinate frame A.

Using the above notations, the assignment of the coordinate frames results in the following transformation matrices between coordinate systems

$$ {}^{A_i}T_{B_i} = \begin{bmatrix} \cos\alpha_i & -\sin\alpha_i & l_i \\ \sin\alpha_i & \cos\alpha_i & 0 \\ 0 & 0 & 1 \end{bmatrix} \qquad (1) $$

$$ {}^F T_{Ai} = \begin{bmatrix} \cos\theta_i & -\sin\theta_i & {}^F x_{Ai} \\ \sin\theta_i & \cos\theta_i & {}^F y_{Ai} \\ 0 & 0 & 1 \end{bmatrix}. \qquad (2) $$

The transformation matrices (1) and (2) are applied to determine the position kinematics of the vehicle.

Using (1) and (2), the position of point B_i in the inertial frame F is

$$ \begin{aligned} {}^F p_{B_i} &= {}^F T_{A_i}\, {}^{A_i} T_{B_i}\, {}^{B_i} p_{B_i} \\ &= \begin{bmatrix} \cos\theta_i & -\sin\theta_i & {}^F x_{A_i} \\ \sin\theta_i & \cos\theta_i & {}^F y_{A_i} \\ 0 & 0 & 1 \end{bmatrix} \begin{bmatrix} \cos\alpha_i & -\sin\alpha_i & l_i \\ \sin\alpha_i & \cos\alpha_i & 0 \\ 0 & 0 & 1 \end{bmatrix} \begin{bmatrix} 0 \\ 0 \\ 1 \end{bmatrix} \\ &= \begin{bmatrix} {}^F x_{A_i} + l_i \cos\theta_i \\ {}^F y_{A_i} + l_i \sin\theta_i \\ 1 \end{bmatrix}. \end{aligned} \qquad (3) $$

Using (2), the homogeneous coordinates of the rear reference point R_{1r} associated with the lead vehicle in frame *Fxy* are

$$ {}^F p_{R_{1r}} = {}^F T_{A_1}\, {}^{A_1} p_{R_{1r}} = \begin{bmatrix} {}^F x_{A_1} - L_1 \cos\theta_1 \\ {}^F y_{A_1} - L_1 \sin\theta_1 \\ 1 \end{bmatrix}. \qquad (4) $$

Similarly, the homogeneous coordinates of the front reference point R_{1r} associated with the following vehicle in frame *Fxy* are

$$ {}^F p_{R_{2f}} = {}^F T_{A_{21}}\, {}^{A_2} p_{R_{2r}} = \begin{bmatrix} {}^F x_{A_2} + L_2 \cos\theta_2 \\ {}^F y_{A_2} + L_2 \sin\theta_2 \\ 1 \end{bmatrix}. \qquad (5) $$

2.1.2 Non-holonomic constaraints

If the rotation of the wheels with respect to their proper axes is ignored, the vehicle configuration can be described by four generalized coordinates $q_i=[{}^F x_{Ai}, {}^F y_{Ai}, \theta_i, \alpha_I]^T \in \Re^4$.

Differentiating (3), the components of the velocity of point B_i with respect to the inertial frame *Fxy* and expressed in *Fxy* are

$$ {}^F\dot{p}_{B_i} = \begin{bmatrix} {}^F\dot{x}_{B_i} \\ {}^F\dot{y}_{B_i} \\ 0 \end{bmatrix} = \begin{bmatrix} {}^F\dot{x}_{A_i} - l_i\dot{\theta}_i \sin\theta_i \\ {}^F\dot{y}_{A_i} + l_i\dot{\theta}_i \cos\theta_i \\ 0 \end{bmatrix}. \quad (6) $$

In order to derive the non-holonomic constraints of the front virtual wheel, the velocity of point B_i relative to frame *Fxy* is expressed in frame $B_i x_i y_i$

$$ {}^{B_i}\dot{p}_{B_i} = \begin{bmatrix} {}^{B_i}v_{B_i x_{Bi}} \\ {}^{B_i}v_{B_i y_{Bi}} \\ 0 \end{bmatrix} = \left({}^F T_{A_i}\, {}^{A_i}T_{B_i}\right)^{-1} {}^F\dot{p}_{B_i} $$
$$ = \begin{bmatrix} \cos(\theta_i+\alpha_i) & \sin(\theta_i+\alpha_i) & * \\ -\sin(\theta_i+\alpha_i) & \cos(\theta_i+\alpha_i) & * \\ 0 & 0 & 1 \end{bmatrix} \begin{bmatrix} {}^F\dot{x}_{B_i} \\ {}^F\dot{y}_{B_i} \\ 0 \end{bmatrix} \quad (7) $$

where the terms indicated by (*) are irrelevant in the computation. Based on the assumption of rolling without lateral sliding, one has ${}^{B_i}v_{B_i y_{Bi}} = 0$, where ${}^{B_i}v_{B_i y_{Bi}}$ is the component of the velocity of point B_i along the y_{Bi} axis of frame $B_i x_{Bi} y_{Bi}$. From the second line of equality (7) and by using expressions (6) for ${}^F\dot{p}_{B_i}$, the non-holonomic constraint for the front virtual wheel can be written in the form

$$ 0 = -{}^F\dot{x}_{A_i} \sin(\theta_i+\alpha_i) + {}^F\dot{y}_{A_i} \cos(\theta_i+\alpha_i) + l_i\dot{\theta}_i \cos\alpha_i . \quad (8) $$

Likewise, using (2), the non-holonomic constraint imposed on the rear virtual wheel can be derived from the second line of the following expression

$$ {}^{A_i}\dot{p}_{A_i} = \begin{bmatrix} {}^{A_i}v_{A_i x_{Ai}} \\ {}^{A_i}v_{A_i y_{Ai}} \\ 0 \end{bmatrix} = {}^F T_{A_i}^{-1}\, {}^F\dot{p}_{A_i} $$
$$ = \begin{bmatrix} \cos\theta_i & \sin\theta_i & * \\ -\sin\theta_i & \cos\theta_i & * \\ 0 & 0 & 1 \end{bmatrix} \begin{bmatrix} {}^F\dot{x}_{A_i} \\ {}^F\dot{y}_{A_i} \\ 0 \end{bmatrix}. \quad (9) $$

Expressing the fact that the wheel cannot move in lateral direction (${}^{A_i}v_{A_i y_{Ai}} = 0$), the non-holonomic constraint is derived from second line of (9) as follows

$$ 0 = -{}^F\dot{x}_{A_i} \sin\theta_i + {}^F\dot{y}_{A_i} \cos\theta_i . \quad (10) $$

Combining equations (8) and (10), the vehicle non-holonomic constraints can be written in the form

$$ C_i(q)\,\dot{q}_i = 0 \quad (11) $$

where $C_i(q_i)$ is a *2*x 4 full rank matrix of the form

$$ C_i(q) = \begin{bmatrix} -\sin\theta_i & \cos\theta_i & 0 & 0 \\ -\sin(\theta_i+\alpha_i) & \cos(\theta_i+\alpha_i) & l_i\cos\alpha_i & 0 \end{bmatrix} \quad (12) $$

and $\dot{q}_i$

$$ \dot{q}_i = \begin{bmatrix} {}^F\dot{x}_{A_i} & {}^F\dot{y}_{A_i} & \dot{\theta}_i & \dot{\alpha}_i \end{bmatrix}^T \quad (13) $$

is the vector of generalized velocities. The constraint equation (11) can be converted into an affine driftless control system

$$ \dot{q}_i = D_i(q_i)\,\eta \quad (14) $$

where the columns of the 4x2 matrix $D_i(q_i)$

$$ D_i(q_i) = \begin{bmatrix} \cos\theta_i & 0 \\ \sin\theta_i & 0 \\ \dfrac{\tan\alpha_i}{l_i} & 0 \\ 0 & 1 \end{bmatrix} \quad (15) $$

form a basis of the null space of $C_i(q_i)$. The control input $\eta_i = \left[{}^{A_i}v_{A_i x_{Ai}}, \omega_{\alpha i}\right]^T$ is a ***2*** **x** ***1*** vector of independent quasi-velocities which parameterize the degree of freedom of the system, where ${}^{A_i}v_{A_i x_{Ai}}$ is the velocity of point A_i (the mid-point of the rear virtual wheel) and $\omega_{\alpha i}$ is the steering angular velocity of the front wheel.

Differentiating (4) and using the first two equations of (15) for *i=1*, a kinematic model of the lead vehicle can be written in the form

$$ {}^{F}\dot{p}_{R_{1r}} = \begin{bmatrix} {}^{F}\dot{x}_{R_{1r}} \\ {}^{F}\dot{y}_{R_{1r}} \\ \dot{\theta}_1 \end{bmatrix} = \begin{bmatrix} \cos\theta_1 & L_1 \sin\theta_1 \\ \sin\theta_1 & L_1 \cos\theta_1 \\ 0 & 1 \end{bmatrix} \begin{bmatrix} {}^{A_1}v_{A_1x_{A1}} \\ \omega_1 \end{bmatrix} \quad (16) $$

where $\omega_1 := \dot{\theta}_1$ is the angular velocity of the vehicle.

Similarly, differentiating (5) and using the first two equations of (15) for *i=2*, a kinematic model of the following vehicle is obtained in the form

$$ {}^{F}\dot{p}_{R_{2f}} = \begin{bmatrix} {}^{F}\dot{x}_{R_{2f}} \\ {}^{F}\dot{y}_{R_{2f}} \\ \dot{\theta}_2 \end{bmatrix} = \begin{bmatrix} \cos\theta_2 & -L_2 \sin\theta_2 \\ \sin\theta_2 & L_2 \cos\theta_2 \\ 0 & 1 \end{bmatrix} \begin{bmatrix} {}^{A_2}v_{A_2x_{A2}} \\ \omega_2 \end{bmatrix} \quad (17) $$

where $\omega_2 := \dot{\theta}_2$ is the angular velocity of the vehicle. In this paper, the vehicle angular velocity (the front wheel steering angle α_2, respectively) is considered as a control input instead of the steering angle velocity. From the third equation of (15) for *i=2* , the front wheel steering angle can be expressed in terms of the vehicle angular velocity as follows

$$ \alpha_2 = a\tan\left(l_2 \frac{\dot{\theta}_2}{{}^{A_2}v_{A_2y_{A2}}} \right). \quad (18) $$

2.2 Relative Kinematics

A plan view of a two-vehicle convoy moving on a horizontal plan is shown in Fig.2.

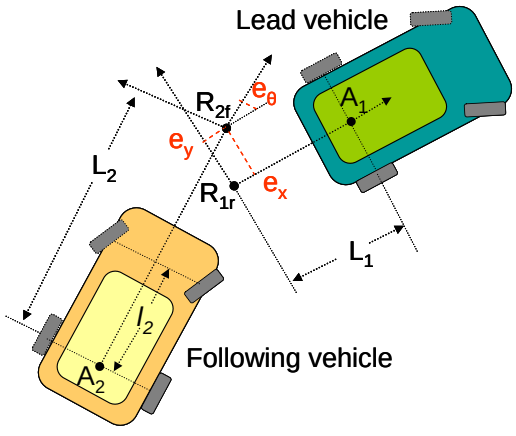

Fig. 2. System configuration for autonomous following

A virtual reference points R_{1r} associated with the lead vehicle is defined on the longitudinal vehicle axle at a distance L_1 behind the rear vehicle axle. A virtual reference point R_{2f} is located on the longitudinal vehicle axle at a distance L_2 in front of the rear vehicle axle of the following vehicle. Two coordinate systems $R_{1r}xy$ and $R_{2f}xy$ whose origins are located at the vehicle reference points R_{1r} and R_{2f}, respectively, (the x-axes are oriented along the longitudinal vehicle axles) are defined to describe the relative position and orientation of the vehicles.

The coordinates and orientation of the frame $R_{2f}xy$ in the coordinates frame $R_{1r}xy$ can be expressed as follows

$$ \begin{bmatrix} e_x \\ e_y \\ e_\theta \end{bmatrix} = \begin{bmatrix} \cos\theta_1 & \sin\theta_1 & 0 \\ -\sin\theta_1 & \cos\theta_1 & 0 \\ 0 & 0 & 1 \end{bmatrix} \begin{bmatrix} {}^{F}x_{R_{2f}} - {}^{F}x_{R_{1r}} \\ {}^{F}y_{R_{2f}} - {}^{F}y_{R_{1r}} \\ \theta_2 - \theta_1 \end{bmatrix} \quad (19) $$

where $e = [e_x,\ e_y, e_\theta]^{\mathrm{T}} \in \Re^3$ is the error posture.

Remark 1: It should be noted that the vehicle-to-vehicle distance and the relative inter-vehicle orientation e_θ are measured by sensors that monitor the rear end of the lead vehicle. Since we know the position and the orientation of the sensors and the frame $R_{2f}xy$ relative to the following vehicle frame $A_2x_{A2}y_{A2}$, as well as the position and the orientation of $R_{1r}xy$ with respect to $A_1x_1y_{A1}$, using geometric argument, we can calculate the position (e_x, e_y) and orientation e_θ of the frame R_{2f} with respect to the coordinate frame R_{1r}. ◊

Differentiating (18) with respect to time and taking into account Eqs. (4) and (5), after some work, the inter-vehicle kinematics in error coordinates is obtained as

$$ \begin{bmatrix} \dot{e}_x \\ \dot{e}_y \\ \dot{e}_\theta \end{bmatrix} = \begin{bmatrix} \cos e_\theta & -L_2 \sin e_\theta \\ \sin e_\theta & L_2 \cos e_\theta \\ 0 & 1 \end{bmatrix} \begin{bmatrix} {}^{A_2}v_{A_2x_{A2}} \\ \omega_2 \end{bmatrix} - \begin{bmatrix} 1 & 0 \\ 0 & -L_1 \\ 0 & 1 \end{bmatrix} \begin{bmatrix} {}^{A_1}v_{A_1x_{A1}} \\ \omega_1 \end{bmatrix} + \dot{\theta}_2 \begin{bmatrix} 0 & 1 & 0 \\ -1 & 0 & 0 \\ 0 & 0 & 0 \end{bmatrix} \begin{bmatrix} e_x \\ e_y \\ e_\theta \end{bmatrix} \quad (20) $$

where $\left({}^{A_1}v_{A_1x_{A1}}, \omega_1\right)$ and $\left({}^{A_2}v_{A_2x_{A2}}, \omega_2\right)$ are the linear and angular velocities of the lead and following vehicle, respectively. From now on, to

simplify the notations, the vehicle linear velocities will be denoted as follows: $v_{A1} := {}^{A_1}v_{A_1x_{A1}}$ and $v_{A2} := {}^{A_2}v_{A_2x_{A2}}$ for the lead and the following vehicle, respectively. The linear and angular velocities of the following vehicle are the control inputs of the system (20).

3 Problem Formulation

One of the challenges in designing controllers for automatic vehicle tracking is to decide on the desired trajectory of the following vehicle. On a curved road section, traveling an arc concentric to that traveled by the lead car but with bigger or smaller radius may be unacceptable from a practical point of view, (for example, the problem of "cutting the corner"), (Fig. 3).

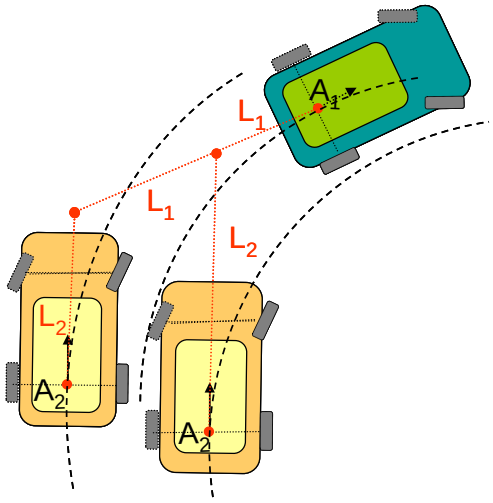

Fig. 3. Circular motion with $L_1 \neq L_2$

Assuming constant velocity maneuvers for forward driving of the lead vehicle, we are interested in a tracking scenario where the two-vehicle convoy will travel concentric arcs of same radii, (Fig. 4), with prescribed inter-vehicle distance depending on the curvature radius of the path taken by the lead vehicle and an *a priori known* desired inter-vehicle spacing, which is defined for the case of straight line driving.

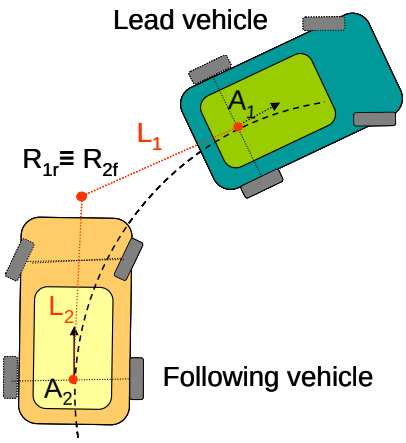

Fig. 4. Circular motion with $L_1 = L_2$

In the case of straight line motion of the lead vehicle, (Fig.5), the *desire inter-vehicle distance* is defined to be:

$$d_{des} = S_1P_2 = 2L - \left(A_1S_1 + P_2B_2 + l_2\right) \quad (21)$$

where $L=L_1=L_2$ is a *known* constant distance determined from consideration of safety driving, sensor requirements, look-ahead visibility during the turning maneuver.

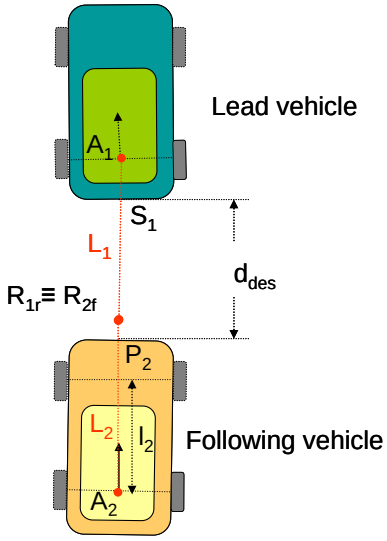

Fig. 5. Desired inter-vehicle spacing

At steady state, the inter-vehicle distance during circular motion of constant radius is a little

smaller, and has different value for different curvature radius of the leader path, and in that way, the requirement of circular motion of same radii is satisfied. Using trigonometric argument, the inter-vehicle distance S_1P_2 at steady state is obtained as follows

$$S_1P_2 = sqrt[2L^2 - 2Lb + b^2 + 2(l-b)L\cos e_{\theta ss}] \quad (22)$$

where $b=l_2 + B_2P_2$. For rectilinear motion of the lead vehicle et steady state, the inter-vehicle orientation is $e_{\theta ss}=0$, and for the inter-vehicle distance S_1P_2 the expression (21) follows readily.

Given the inter-vehicle kinematics in error coordinates (20), and assuming that the linear and angular velocities of the lead vehicle (v_{A1}, ω_1) are unknown constant parameters and are not available for feedback control, the *control objectiv*e is to asymptotically track the virtual reference point R_{1r} the lead vehicle with the reference point R_{2f} of the following vehicle.

4 Adaptive Control Design

First, we consider the problem of controlling the motion of the following vehicle during constant velocity maneuvers for forward driving of the lead vehicle. Since the leader velocities are not available for feedback control design, we propose an adaptive control law, which achieves asymptotic stabilization of the closed-loop system in error coordinates. The control velocities of the following vehicle are computed using the leader velocity estimates $(\hat{v}_{A1}, \hat{\omega}_1)$ obtained from the dynamic (adaptive) part of the proposed controller. For this purpose, let us consider the following change of inputs in (20)

$$\begin{bmatrix} u_1 \\ u_2 \end{bmatrix} = \begin{bmatrix} \cos e_\theta & -L_2 \sin e_\theta \\ \sin e_\theta & L_2 \cos e_\theta \end{bmatrix} \begin{bmatrix} v_{A2} \\ \omega_2 \end{bmatrix}. \quad (23)$$

One easy verifies that the transformation matrix in (23) is nonsingular when $L_2 \neq 0$.

Using the input transformations (23), the inter-vehicle kinematic equations in error coordinates (20) can be written in the form

$$\begin{aligned} \dot{e}_x &= -v_{A1} + \omega_1 e_y + u_1 \\ \dot{e}_y &= (L_1 - e_x)\omega_1 + u_2 \\ e_\theta &= -\omega_1 + \left(-u_1 \frac{\sin e_\theta}{L_2} + u_2 \frac{\cos e_\theta}{L_2} \right) \end{aligned} \quad (24)$$

The adaptive control design is based on a reduced-order system composed of the first two equations of (24)

$$\begin{aligned} \dot{e}_x &= -v_{A1} + \omega_1 e_y + u_1 \\ \dot{e}_y &= (L_1 - e_x)\omega_1 + u_2 \end{aligned} \quad (25)$$

Consider the subsystem (25) and assume that the leader velocities $v_{A1} = cte > 0$ and $\omega_1 = cte$, are unknown constant parameters. The *control problem* consists in finding an adaptive feedback control law for the system (25) with inputs (u_1, u_2) such that

$$\lim_{t\to\infty}(e_x(t)) = 0 \text{ and } \lim_{t\to\infty}(e_y(t)) = 0. \quad (26)$$

Assume that $L_2 \neq 0$ and consider the control

$$\begin{aligned} u_1 &= -k_x e_x + \hat{v}_{A1} - \hat{\omega}_1 e_y \\ u_2 &= -k_y e_y - (L_1 - e_x)\hat{\omega}_R \end{aligned} \quad (27)$$

where k_x and k_y are positive gains. We consider the following Lyapunov function candidate

$$V = \frac{1}{2}e_x^2 + \frac{1}{2}e_y^2 + \frac{1}{2\gamma_v}\tilde{v}_{A1}^2 + \frac{1}{2\gamma_\omega}\tilde{\omega}_1^2 \quad (28)$$

where $\tilde{v}_{A1}$ and $\tilde{\omega}_1$ are the parameter errors

$$\begin{aligned} \tilde{v}_{A1} &= \hat{v}_{A1} - v_{A1} \\ \tilde{\omega}_1 &= \hat{\omega}_1 - \omega_1 \end{aligned} \quad (29)$$

and $\gamma_v = cte > 0$, and $\gamma_\omega = cte > 0$ are the adaptation gains.
Using (29), the derivative of V is obtained in the form

$$\begin{aligned} \dot{V} = -k_x e_x^2 - k_y e_y^2 + \tilde{v}_{A1}\left(e_x + \frac{1}{\gamma_v}\dot{\tilde{v}}_{A1}\right) \\ + \tilde{\omega}_1\left[-e_x e_y - e_y(L_1 - e_x) + \frac{1}{\gamma_\omega}\dot{\tilde{\omega}}_R \right] \end{aligned} \quad (30)$$

where all the terms containing $\tilde{v}_{A1}$, as well as $\tilde{\omega}_1$, have been grouped together. To eliminate them, the update law is chosen as

$$\begin{aligned} \dot{\hat{v}}_{A1} &= -\gamma_v e_x \\ \dot{\hat{\omega}}_1 &= \gamma_\omega L_1 e_y \end{aligned} \quad (31)$$

and the derivative of V is obtained as

$$\dot{V} = -k_1 e_x^2 - c_1 e_y^2 \leq 0 . \qquad (32)$$

The resulting closed-loop adaptive system in error coordinates becomes

$$\begin{aligned} \dot{e}_x &= -k_x e_x + \tilde{v}_{A1} - e_y \tilde{\omega}_1 \\ \dot{e}_y &= -k_y e_y - (L_1 - e_x)\tilde{\omega}_1 \\ \dot{\tilde{v}}_{Rx} &= -\gamma_v e_x \\ \dot{\tilde{\omega}} &= -\gamma_\omega L_1 e_y \end{aligned} . \qquad (33)$$

Proposition 1: Assume that lead vehicle linear and angular velocities (v_{A1}, ω_1) are bounded unknown constant parameters, $v_{A1} > c_v = cte > 0$ and $L_1 \neq 0$. If the control law given by (27) is applied to (25) where the lead vehicle velocity estimates $(\hat{v}_{A1}, \hat{\omega}_1)$ are obtained from the parameter update law (31), the origin $x = [e_x, e_y, \tilde{v}_{A1}, \tilde{\omega}_1]^T = 0$ of the closed-loop system in error coordinates (33) is asymptotically stable.

Proof. The system has an equilibrium point at the origin. The function (28) is continuously differentiable and positive definite. From (32), it follows that (28) is non-increasing, ($V(t) \leq V(0)$), and this in turn implies that $e_x(t), e_y(t), \tilde{v}_{A1}(t)$ and $\tilde{\omega}_1(t)$ are uniformly bounded with respect to the initial conditions. By application of the LaSalle-Yoshizawa Theorem [17, p.24, Theorem 2.1],

$$\lim_{t \to \infty} \dot{V} = -k_1 e_x^2 - c_1 e_y^2 = 0 . \qquad (34)$$

Therefore

$$e_x(t) \to 0,\ e_y(t) \to 0 \qquad (35)$$

as $t \to \infty$. From the third and forth equations of (33), it follows that $\dot{\tilde{v}}_{Rx} \to 0, \dot{\tilde{\omega}}_R \to 0$ as $t \to \infty$.

The first equation of (33) can be seen as a derivative of a differentiable function $e_x(t)$ from R^+ to R, which converges to limit value (0) when t tends to infinity, and its derivative, (the right side of this equation) can be seen as a sum of two terms, one, ($\tilde{v}_{A1}$), being uniformly continuous since its derivative is bounded, and the other, ($-k_x e_x - e_y \tilde{\omega}_1$), which tends to zero. By application of the extended version of Barbalat's Lemma [18], it follows that $\dot{e}_x(t) \to 0$ as $t \to \infty$, and this in turn implies that the term

$$\tilde{v}_{Rx} \to 0 \qquad (36)$$

as $t \to \infty$.

In the same fashion, it can be proved from the second equation of (33) that $\dot{e}_y(t) \to 0$ as $t \to \infty$ and this in turn implies that the term

$$\tilde{\omega}_R \to 0 . \qquad (37)$$

Since the dynamics of e_θ has not been taken into account into the feedback control design, the next step in the stability analysis is to establish asymptotic convergence of e_θ to the equilibrium state $e_{\theta ss}$ which depends of lead vehicle linear and angular velocities (v_{A1}, ω_1), or equivalently the curvature radius of the path driven by the lead vehicle $\rho_R = v_{A1}/\omega_1$, and the distances L_1 and L_2. We analyze the zero dynamics of e_θ assuming that $e_x(t) \equiv 0; e_y(t) \equiv 0$ and $\tilde{v}_{A1} \equiv 0; \tilde{\omega}_1 \equiv 0$ for all time. In this case, substituting (27) into the third equation of (24) after some work, the zero dynamics of e_θ is obtained as

$$\dot{e}_\theta = -\frac{v_{A1}}{L_2} \sin e_\theta - \omega_1 \left(1 + \frac{L_1}{L_2}\right) \cos e_\theta . \qquad (38)$$

Since we are interested in tracking scenario where at steady state the vehicle convoy will travel concentric arcs of same radii, we assume that $L_1 = L_2 = L$. Using the transformation

$$\Phi := \tan(e_\theta / 2) \qquad (39)$$

equation (38) can be rewritten in the form

$$\dot{\Phi} = -\frac{v_{A1}}{L} \Phi - \omega_1 . \qquad (40)$$

Equation (40) represents first order linear differential equation with constant coefficients. The solution of (41) with initial condition $\Phi(0) = 0$ is given in the form

$$\Phi(t) = \frac{L \omega_1}{v_{A1}} \left[\exp(-\frac{v_{A1}}{L} t) - 1 \right] . \qquad (41)$$

From (41), it can be seen that

$$\Phi(\infty) = -\frac{L\,\omega_1}{v_{A1}} = \Phi_{ss} = cte\ . \qquad (42)$$

Using the inverse transformation of (39), the relative orientation of the vehicles at steady state $e_{\theta ss}$ is obtained as

$$e_{\theta ss} = 2a\tan(l/\rho_R) = cte \qquad (43)$$

where

$$\rho_R = v_{A1}/\omega_1 = cte \qquad (44)$$

is the curvature radius of the path travel by the lead vehicle. Since $e_x = e_y = 0$, i.e., the reference points R_{1r} and R_{2f} coincide, and $L_1 = L_2 = L$, using geometrical argument, it follows that the two vehicles will travel concentric arcs of same radii**,** which complete the proof. □

Remark 2: In addition to Proposition 1, based on the linearization at the origin of the system (33), it can be shown that

$$x = [e_x, e_y, \tilde{v}_{A1}, \tilde{\omega}_1]^T = 0 \qquad (45)$$

is an exponentially stable equilibrium point for the corresponding linear system. Using [19, Theorem 3.11, p.147], we conclude that the proposed adaptive control law achieves local exponential stability of x=0 for the nonlinear system. ◊

Using the inverse transformations of (23) and expressions (27) for the control inputs (u_1, u_2), we obtain expressions for the actual control inputs (v_{A2}, ω_2) and in turn, from (18), for the front wheel steering angle α_2 of the following vehicle.

Remark 3: The adaptive control law designed in this Section, is based on the assumption of unknown *constant* linear and angular velocities of the lead vehicle. It is very interesting to analyze the performance of the proposed controller, if the lead vehicle velocities are *time-varying* parameters, and assuming that their derivatives are bounded. In this case, the resulting closed-loop adaptive system in error coordinates (33) becomes

$$\begin{aligned}
\dot{e}_x &= -k_x e_x + \tilde{v}_{A1} - e_y\tilde{\omega}_1 \\
\dot{e}_y &= -k_y e_y - (L_1 - e_x)\tilde{\omega}_1 \\
\dot{\tilde{v}}_{Rx} &= -\gamma_v e_x - \dot{v}_{A1} \\
\dot{\tilde{\omega}} &= -\gamma_\omega L_1 e_y - \dot{\omega}_1
\end{aligned} \qquad (46)$$

The closed-loop system can be written in vector form as

$$\dot{x} = f(x) + g(t)\,. \qquad (47)$$

The system (47) can be seen as a perturbation of the nominal system (33). The perturbation term $g(t)$

$$g(t) = \begin{bmatrix} 0 \\ 0 \\ \dot{v}_{A1} \\ \dot{\omega}_1 \end{bmatrix} \qquad (48)$$

is assumed to be an uniformly bounded disturbance that satisfies $\|g(t)\| \le \delta = cte$, for all $t \ge 0$, which is reasonable assumption from a practical view point, since the lead vehicle velocities are always bounded due to physical limitations imposed on the driving and steering abilities of the vehicle.

In this case, since the nominal system is exponentially stable, /Remark 2/, by using [19, Theorem 5.1, page 211], it can be shown that $x(t)$ will be ultimately bounded.

In addition, when $\|g(t)\| \to 0$, that is, the lead vehicle velocities converge to some constant values, by using [19, Lemma 5.2, page 213], it can be shown that the solution of the perturbed system (47)

$$x(t) \to 0 \quad \text{as} \quad t \to \infty. \qquad (49)$$

◊

5 Simulation Results

To illustrate the effectiveness of the proposed controller, several simulations are carried out in order to evaluate the vehicle behavior and tracking accuracy. In the simulation using MATLAB, a planar bicycle 2DOFs vehicle model was used. The longitudinal vehicle base was chosen to be $l_1=l_2=l = 2m$. For simplicity in the simulation, we set $l = P_2A_2$ and $A_1S_1 = 0$, (Fig. 5). The distance $L = L_1 = L_2$ was chosen to be $L=4m$, which corresponds to desired inter-vehicle separation $d_{des}=6m$ in the case of straight line motion of the lead vehicle, (Fig. 6). The gains in the control law (27) were chosen as $k_x = 8$; $k_y = 20$; $\gamma_v = 5$; $\gamma_\omega = 0.5$. The initial position and orientation of the following vehicle in the inertial frame Fxy were chosen to be ${}^F x_{A2}(0) = 0m$, ${}^F y_{A2}(0) = 0m$, $\theta_2(0) = 0rad$. The initial position and orientation of the lead vehicle in the inertial frame Fxy were chosen to be ${}^F x_{A1}(0) = 9.3\ m$, ${}^F y_{A1}(0) = 0$, $\theta_1(0) = -\ 0{,}25rad$. In this case, the initial inter-

vehicle distance $S_1P_2 = 7.37m$ which is different from d_{des}. The initial values of the error coordinates were $e_x(0) = 1m$; $e_y(0) = -1m$; $e_\theta(0) = -0.25rad$. The initial estimates for the leader linear and angular velocities were chosen to be $\hat{v}_{A1}(0) = 2m/s$ and $\hat{\omega}_1(0) = 0rad/s$, and are different from the real values of the lead vehicle velocities ($v_{A1} = 4m/s$, $\omega_1 = 0.27rad/s$) for the first maneuver (Table I). The leader path consists of three consecutive constant velocity maneuvers: turning both to the left and to the right followed by a straight line motion. The corresponding actual lead vehicle velocities are given in Table 1.

Table 1

	Radius of turn ρ_R [m]	Duration [s]	Leader linear velocity v_{A1} [m/s]	Leader angular velocity ω_1 [rad/s]
Maneuver 1 - left turn	*15*	*10*	*4*	*0.27*
Maneuver 2 -right turn	*10*	*22*	*2*	*-0.2*
Maneuver 3 - straight line	-	*8*	*5*	*0*

- In the first simulation, from Fig. 6, we can see the planar paths drown by the vehicle guide points A_1 and A_2 of the lead and following vehicle, respectively, (the mid-points of the rear vehicle axles). At steady state, the following vehicle tracks the path taken by the lead vehicle without lateral error.

From Fig. 7, we can see the evolution in time of the error coordinates. For each maneuver, the position errors $e_x(t)$ and $e_y(t)$ tend asymptotically to zero, i.e., at steady state, the look-ahead virtual point R_{2f} coincides with the virtual reference point R_{1r}. The inter-vehicle orientation $e_\theta(t)$ tends also asymptotically to a constant value $e_{\theta ss}$.

As shown in Fig. 8, the estimates of the leader velocities tend asymptotically to their actual values.

From Fig. 9, we can see the evolution in time of the inter-vehicle distance S_1P_2. The steady-state inter-vehicle distance during circular motion of constant radius is different for different values of the curvature radius of the leader path For example, for the first maneuver ($\rho_R = 15m$), at steady state $S_1P_2 = 5.82m$; for the second maneuver ($\rho_R = 10m$), at steady state $S_1P_2 = 5.62m$ and are a little smaller compared to the desired distance d_{des} of $6m$ during the straight line motion. In that way, the requirement of circular motion of same radii of the vehicles is satisfied. This is in accordance with the theoretical result obtained in Section IV.

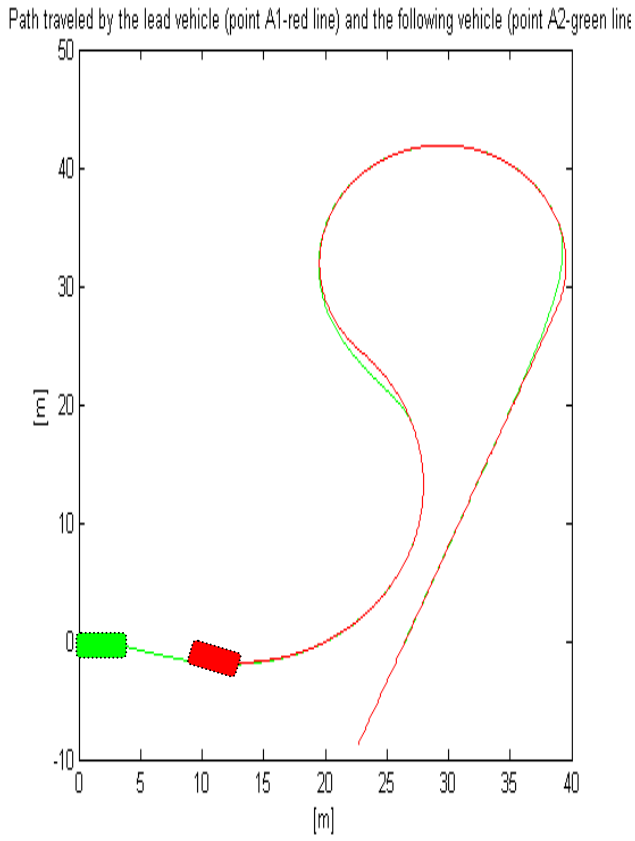

Fig. 6. A planar path drown by the vehicle guide points (the mid-points of the rear vehicle axles); red line (point A_1, lead vehicle), green line (point A_2, following vehicle), $L_1 = L_2 = 4m$; $d_{des} = 6m$

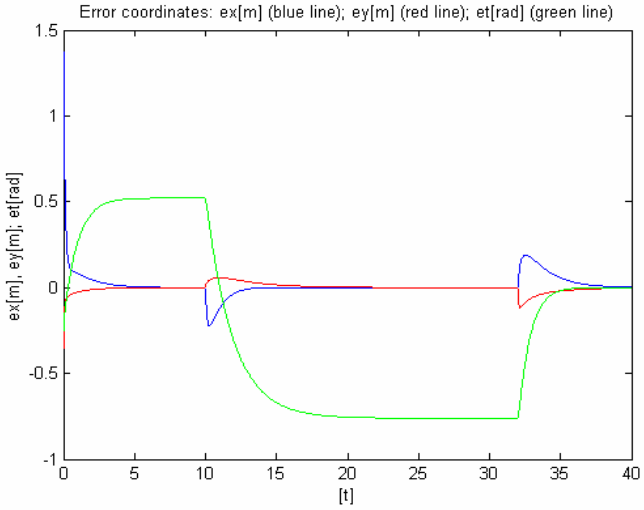

Fig. 7. Evolution of the error coordinates in time: $e_x(t)$ (blue line); $e_y(t)$ (red line); $e_\theta(t)$ (green line); $L_1 = L_2 = 4m$; $d_{des} = 6m$

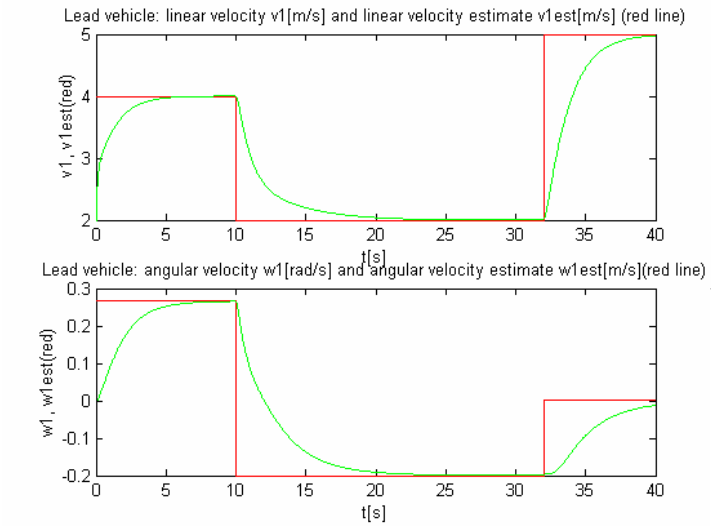

Fig. 8. Evolution in time of the lead vehicle velocities estimates $(\hat{v}_{A1}, \hat{\omega}_1)$ (green line); lead vehicle actual velocities v_{A1} and ω_1 (red line); $L_1 = L_2 = 4m$; $d_{des} = 6m$

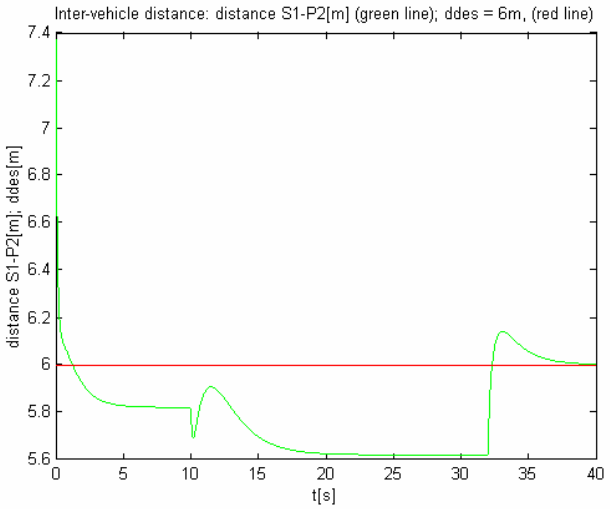

Fig. 9. Evolution of the inter-vehicle distance S_1P_2 in time (green line); Desired inter-vehicle distance during straight line motion of the leader: $d_{des} = 6m$ (red line); $L_1 = L_2 = 4m$

- In order to demonstrate the scenario when at steady tate, the two vehicle travel concentric arc with different radii (the problem of "cutting the corner"), in the second simulation, we set $L_1 = 2m$ and $L_2 = 6m$. The desired inter-vehicle distance for a straight line motion $d_{des} = 6m$ is the same, as in the first simulation. All other conditions, (lead vehicle velocities, curvature radii ρ_R, the initial estimates for the leader linear and angular velocities, initial position coordinates and orientation in the inertial frame, and the initial values of the error coordinates) were the same as in the first simulation. The problem of "cutting the corner" ,i.e., traveling an arc *concentric* to that traveled by the lead car but with smaller radius clearly appears in Fig. 10.

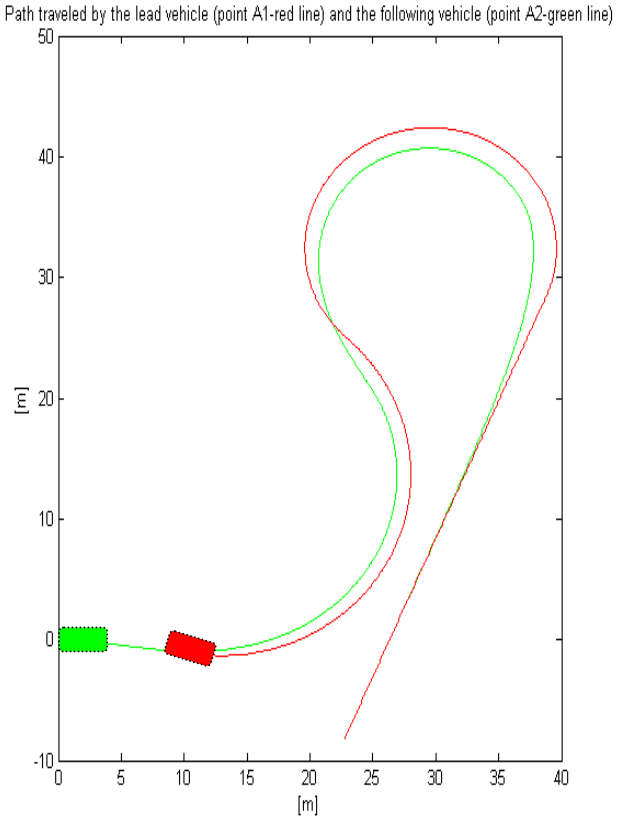

Fig. 10. A planar path drown by the vehicle guide points (the mid-points of the rear vehicle axles); red line (point A_1, lead vehicle), green line (point A_2, following vehicle), $L_1 = 2m$ and $L_2 = 6m$, $d_{des} = 6m$

For example, during the second maneuver of the lead vehicle, at steady state, the curvature radius of *8.3m* for the path traveled by the following vehicle is much smaller compared to the curvature radius of the path traveled by the lead vehicle ($\rho_R = 10m$). which results in a error of $\Delta\rho = 1.7m$, which may be unacceptable from a practical point of view. In order to obtain *smaller* error between the curvature radii of the concentric arcs traveled by the two vehicles when $L_1 \neq L_2$, we have to assign smaller desired inter-vehicle separation d_{des} in the case of straight line motion of the lead vehicle.

- In the third simulation, we simulate the performance of the proposed controller when the lead vehicle velocities during the second and the third maneuver are *time-varying* parameters given in Table 2. All the initial conditions as well as the distances $L_1 = L_2 = 4m$ are as in the first simulation.

Table 2

	Radius of turn ρ_R [m]	Dura-tion [s]	Leader linear velocity v_{A1} [m/s]	Leader angular velocity ω_1 [rad/s]
Maneuver 1 - left turn	*15*	*10*	*4*	*0.27*
Maneuver 2 - right turn	*10*	*22*	*2+0.2sin(0.2 t)*	*-0.2*
Maneuver 3 - straight line	-	*8*	$5-3e^{-0.2t}$	*0*

We can see from Fig. 11, 12, 13 and 14 that all the signals are bounded (during the second maneuver) which is in conformity with the theoretical results obtained in Section IV. We note that, if the lead vehicle linear velocity converges to a constant value (which is the case during the third maneuver), the velocity estimate converges to this constant value, (Fig. 11).

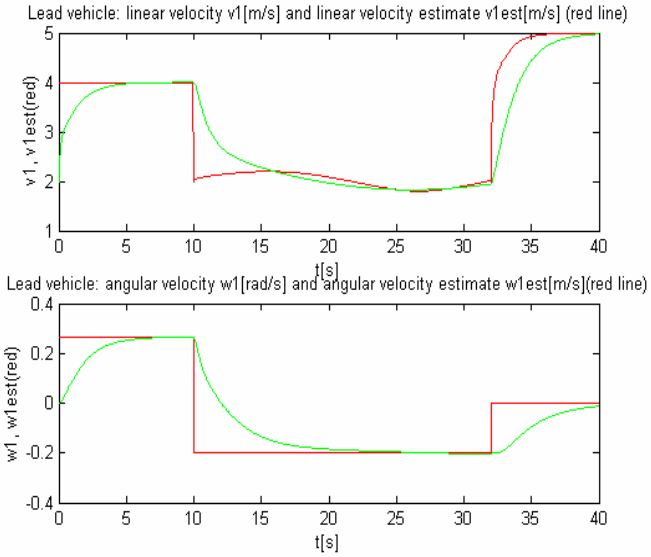

Fig. 11. Evolution in time of the lead vehicle velocities estimates $(\hat{v}_{A1}, \hat{\omega}_1)$ (green line); lead vehicle actual velocities v_{A1} and ω_1 (red line); $L_1 = L_2 = 4m$; $d_{des} = 6m$

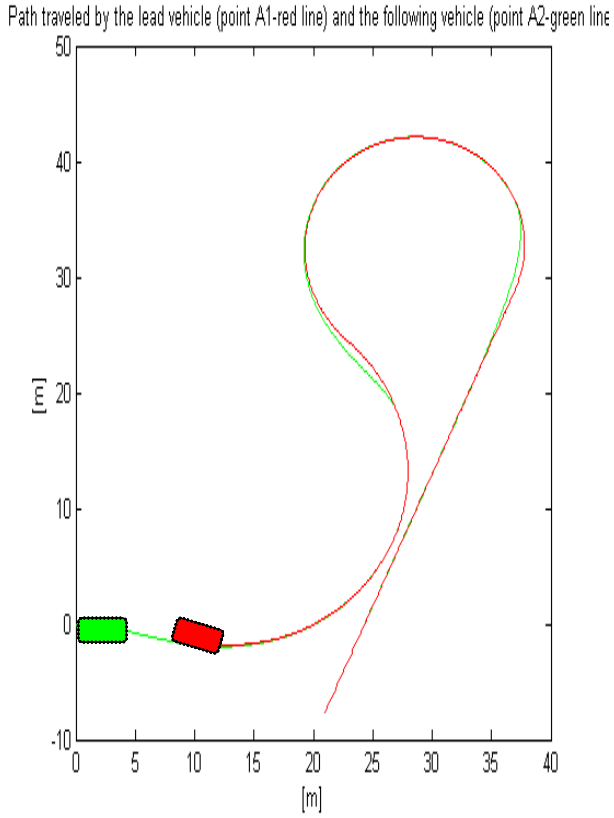

Fig. 12. A planar path drown by the vehicle guide points (the mid-points of the rear vehicle axles); red line (point A_1, lead vehicle), green line (point A_2, following vehicle); $L_1 = L_2 = 4m$; $d_{des} = 6m$

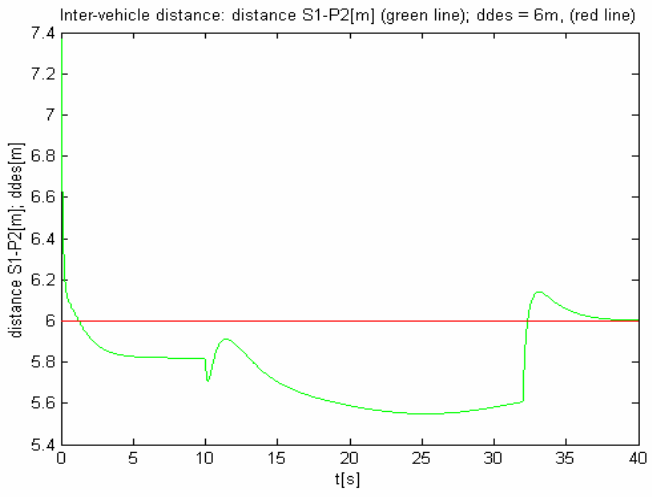

Fig. 13. Evolution of the inter-vehicle distance S_1P_2 in time (green line); Desired inter-vehicle distance during straight line motion of the leader: $d_{des} = 6m$ (red line), $L_1 = L_2 = 4m$

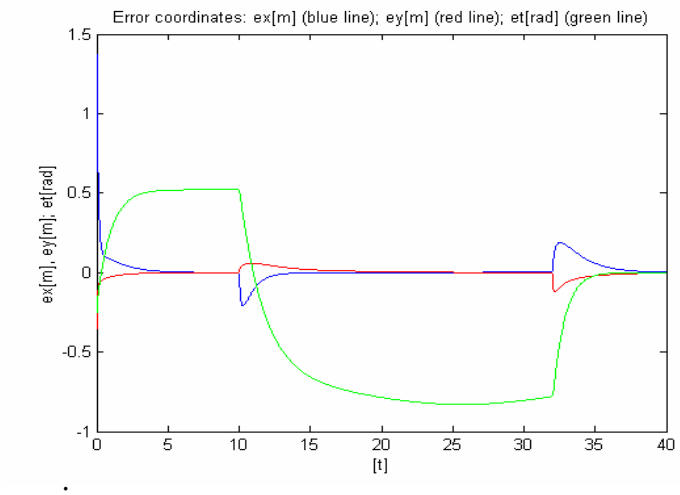

Fig. 14. Evolution of the error coordinates in time: $e_x(t)$ (blue line); $e_y(t)$ (red line); $e_\theta(t)$ (green line), $L_1 = L_2 = 4m$; $d_{des} = 6m$

The results of the simulation verify the validity of the proposed controller.

6 Conclusion

This paper considers the problems of kinematic modeling of a two-vehicle convoy and the design of a vehicle following controller that tracks the trajectory of the vehicle ahead with prescribed inter-vehicle distance. It is shown that the use of standard robotic methodology by using homogeneous transformation matrices can be used effectively for modeling the dynamics of the system. In this paper, a systematic method is developed for the design of an adaptive tracking controller for vehicle following. The control problem is solved alike trajectory tracking by coupling lateral and longitudinal control. A specific feature of the control scheme is that it allows the vehicle to follow the car instead of the road, i.e., a strategy for autonomous control was presented without the use of road infrastructure or inter-vehicle communication. The linear and angular velocities of the lead vehicle are unknown constant parameters, and the curvature radius of the lead vehicle path is also unknown. The proposed adaptive control law achieves asymptotic stabilization of the closed-loop system in error coordinates. Assuming constant velocity maneuvers of the leader, at steady state, the following vehicle will track the path taken by the lead vehicle. In that way, the problem of "cutting the corner" has been overcome.

If the lead vehicle velocities are *time-varying* parameters, the proposed controller achieves ultimate boundness of the closed-loop system in error coordinates. In practice, the lead vehicle velocities are always bounded due to physical limitations imposed on the driving and steering abilities of the vehicle, which makes the proposed controller usable for practical implementation. The results of the simulation verify the validity of the proposed controller. Future research will address the problem of a unified approach to control for backward and forward driving of an autonomous convoy with time-varying velocities.

Acknowledgment

This work was supported by National Ministry of Science and Education of Bulgaria under contract BY-I-302/2007: "Audio-video information and communication system for active surveillance cooperating with a Mobile Security Robot".

References:

[1] K. Cheok, G. Smidt, K. Kobayashi, J. Overholt, P. Lescoe, A fuzzy logic intelligent control system paradigm for an in-line-of-sight leader-following HMMWV, *Journal of Robotic Systems*, 14(6), 1997, pp. 407-420.

[2] B. Brumitt, M. Hebert, Experiments in autonomous driving with concurrent goals and multiple vehicles, *Proc. IEEE Int. Conf. Rob. Automation*, 1998, pp.1895-1902.

[3] R. Hogg, A. Rankin, M. McHenry, D. Helmick C. Bergh, S. Roumeliotis, L. Matthies, Sensors and actuators for small robot leader/follower behavior, *15th AeroSense Symposium*, April, 2001.

[4] H. Fritz, Longitudinal and lateral control of heavy duty trucks for automated vehicle following in mixed traffic: experimental results from the CHAUFFEUR project, *Proc. Int. Conf. Contr. Applications*, 1999, pp. 1348-1352.

[5] M.Parent, P.Daviet, Automated urban vehicles: towards a dual mode PRT (Personal Rapid Transit), *Proc. IEEE Conf. Rob. Automation*, 1996, pp.3129-3133.

[6] G. Lu, J. Huang, M. Tomizuka, *Vehicle lateral control under fault in front and/or rear sensors: final report* , Research Report, UCB-ITS-PRR-2004-36.

[7] R. White, M. Tomizuka, Autonomous following lateral control of heavy vehicles

using laser scanning radar, *Proc. American Control Conference*, 2001, pp. 2333-2337.

[8] P. Petrov, M. Parent, An Adaptive Tracking Controller for Backward Driving of a Two-Vehicle Convoy, *Proc. 9th IEEE Int. Conf. Intel. Transport. Systems* (*IEEE ITSC'06*), 2006, pp.1376-1381.

[9] D. Yanakiev, I. Kanellakopoulos, Nonlinear spacing policies for Automated Heavy-Duty Vehicles, *IEEE Trans. Vehicular Technology* Vol. 47, No 4, Nov. 1998, pp. 1365-1377.

[10] S. Shladover, C. Desoer, J. Hedrik, M. Tomizuka, J. Warland, Automatic vehicle control developments in the PATH program, *IEEE Trans. Vehicular Technology*, Vol. 40, No 1 1991, pp. 114-130.

[11] T. Fujioka, M. Omae, Vehicle following control in lateral direction for platooning, *Veh. Syst. Supplement*, 28, 1998, pp. 422-437.

[12] P. Petrov, O. Boumbarov, Nonlinear Adaptive Control of a Two-Vehicle Autonomous Convoy Using a Look-Ahead Approach, *Proc. 7th WSEAS Int. Conf. Signal processing, Robotics and Automation,* (*ISPRA'08*), 2008, pp. 55-60.

[13] M. Pham, D. Wang, A Unified nonlinear controller for a platoon of car-like vehicles, *Proc. Amer. Contr. Conference*, 2004, pp. 2350- 2355.

[14] J. Bom, B. Thuilot, F. Marmoiton, P. Martinet, Nonlinear control for urban vehicle platooning, relying upon a kinematic GPS, *Proc. IEEE Int.Conf. Rob. Automation*, 2005, pp. 4149-4154.

[15] P. Petrov, J. de Lafontaine, M. Tétreault, Hybrid Feedback Control for the Parking Problem of a Load-Haul-Dump Mine Vehicle *Proc. IEEE/RSJ Int. Conf. Intel. Rob. Systems, (IROS'98)*, 1998, pp. 1907-1912.

[16] M. Spong, M. Vidyasagar, *RobotDynamics and control*, John Wiley&Sons, 1988.

[17] M. Kristic, I. Kanellakopoulos, P. Kokotovic, *Nonlinear and Adaptive Control Design*, Wiley, New York, 1995.

[18] C. Samson, Control of chained systems: Application to path following and time-varying point stabilization of mobile robots, *IEEE Trans. Automat. Control*, Vol.40, No1, 1995, pp.64-75.

[19] H. Khalil, *Nonlinear Systems*, Prentice Hall, 1996.